

Hidden Markov and semi-Markov models

When and why are these models useful to classify states
in time series data?

Sofia Ruiz-Suarez^{1,2}, Vianey Leos-Barajas^{3,4}, and Juan Manuel Morales¹

¹INIBIOMA (CONICET-Universidad Nacional del Comahue), Quintral
1250, Bariloche, Rio Negro, Argentina

²Universidad de Rosario, Facultad de Ciencias Económicas, Bv. Oroño
1261, Rosario, Argentina

³Department of Statistical Sciences, University of Toronto, 700 University
Ave, Toronto, ON, M5G 1Z5, Canada

⁴School of the Environment, University of Toronto, 33 Wilcocks St,
Toronto, ON, M5S 3E8, Canada

Abstract

Hidden Markov models (HMMs) and their extensions have proven to be powerful tools for classification of observations that stem from systems with temporal dependence as they take into account that observations close in time to one another are likely generated from the same state (i.e. class). In this paper, we provide details for the implementation of four models for classification in a supervised learning context: HMMs, hidden semi-Markov models (HSMMs), autoregressive-HMMs and autoregressive-HSMMs. Using simulations, we study the classification performance under various degrees of model misspecification to characterize when it would be important to extend a basic HMM to an HSMM. As an application of these techniques we use the models to classify accelerometer data from Merino sheep to distinguish between four different behaviors of interest. In particular in the field of movement ecology, collection of fine-scale animal movement data over time to identify behavioral states has become ubiquitous, necessitating models that can account for the dependence structure in the data. We demonstrate that when the aim is to conduct classification, various degrees of model misspecification of the proposed model may not impede good classification performance unless there is high overlap between the state-dependent distributions.

Keywords— animal behaviour, classification, movement ecology, temporal dependence.

1 Introduction

The aim in the classification problem is either to allocate data to different groups of interest, or to discover sets of patterns that reflect important dynamics of interest. For systems that exhibit temporal dependence, the goal is to correctly assign different segments of data to a finite set of groups, taking into account that observations near each other (in time) are likely to correspond to the same group. For example, in computational linguistics the goal is to identify words and phrases in spoken language, i.e speech recognition (Juang and Rabiner, 1991; Deng and Li, 2013); in meteorology, weather change can be monitored analyzing sequential measures from meteorological radars (Rico-Ramirez and Cluckie, 2008; Ruiz-Suarez et al., 2019); in neurophysiology, different brain activities can be distinguished assessing physiological variables such as heart rate or electrocardiograms through time(Cheng and Chan, 1998; Inan et al., 2006); and in ecology a set of

biologically relevant animal behaviors can be identified from observed acceleration data (Nathan et al., 2012; Leos-Barajas et al., 2017).

In ecology, a lot of attention has been paid to understand and model animal movement (Mevin B. Hooten et al., 2017), as it plays important roles in the fitness and evolution of species(Nathan, 2008), the structuring of populations and communities (Morales et al., 2010), and responses to environmental change (Jonsen, 2016). In order to understand how animals move as they respond to internal conditions and external environments, it is essential to be able to distinguish between a set of biologically relevant behaviors. Tri-axial acceleration (ACC) data is now commonly recorded using biologging devices, allowing researchers to investigate the performance, energy expenditure, and behaviour of free-living animals (Williams et al., 2020). These devices measure the change in speed over time in three directions, which can be described relative to the body of the individual. With this information it is possible to identify different activity patterns to then distinguish between different behaviours (Wilson et al., 2008; Williams et al., 2015).

There are several techniques used to solve classification problems (Trevor Hastie et al., 2001): classification trees, logistic regression, discriminant analysis, neural networks, boosted regression trees, random forests, deep learning methods, nearest neighbors, support vector machines, etc. To classify animal behaviour from accelerometer data many of these techniques have been proposed. For example, (Nathan et al., 2012) identified behavioral modes of griffon vultures using a selection of nonlinear and decision tree methods; (Carroll et al., 2014) trained a support vector machine to classify penguin behaviour as either ‘prey handling’ or ‘swimming’; (Williams et al., 2015) examined the ability of k-nearest neighbour algorithms to distinguish between flight behaviours of Andean condors and griffon vultures; (Chakravarty et al., 2019) developed an hybrid model combining biomechanical features and support vector machines to identify between four possible behaviours of Kalahari Meerkats; and (Studd et al., 2019) used a random forest algorithm and a manually created decision tree to associate observed behaviors of North American red squirrels with logger recorded acceleration and temperature. All these methods assume that the observations are independent, yet time series data presents sequential correlation. This characteristic of the data can be exploited to improve the prediction accuracy of the classifiers (Geurts, 2001; Dietterich, 2002).

The class of hidden Markov models (HMMs) (Zucchini et al., 2017; Frühwirth-Schnatter et al., 2019) provide an intuitive framework for the classification of systems with temporal dependence that experience changes in patterns over time connected with underlying shifts in a latent process of

interest. HMMs assume that the observation(s) at each point in time are the result of the unknown (hidden) ‘state’ (or class) of the system of interest. The state of the system is assumed to evolve over time according to the Markov property, i.e. the conditional probability distribution of future states (conditional on both past and present states) depends only upon the present state. Thus, an HMM is defined as a doubly stochastic process composed of an observation process Y_t and a (latent) state process C_t , where the state process is usually taken to be a first-order Markov chain and we take $X_i \perp X_j | C_t$. As such, HMMs provide a clear manner in which to do classifications of processes that evolve over time, as they take into account the sequential dependence present in the data and the temporal structure of the consecutive states. HMMs have successfully been implemented to classify accelerometer data: (Li et al., 2010) utilized an HMM to recognize human physical activities using two-second summary features from tri-axial acceleration data; (Wang et al., 2011) presented an HMM to recognize six human daily activities from sensor signals collected from a single waist-worn tri-axial accelerometer; (Leos-Barajas et al., 2017) provided the details necessary to implement and assess an HMM in both the supervised and unsupervised learning context and outlined two applications to marine and aerial systems (shark and eagle) taking the unsupervised learning approach.

HMMs are models mostly formulated in discrete time, and as the state process is assumed to be a first order Markov chain, the number of consecutive time points that the system spends in a given state (sojourn time), follows a geometric distribution (Zucchini et al., 2017; Langrock and Zucchini, 2011). The popularity of HMMs stems, in part, from the ease with which they can be extended to accommodate other forms of dependence and structures. For instance, the state-duration distribution can be generalized so that the underlying stochastic process is a semi-Markov chain. These models are called hidden semi Markov models (HSMM) (Yu, 2010), and by being more flexible they allow more realism, improving the classifications when the sojourn time distributions are far from being geometric. HSMMs have been successfully applied in many areas, mostly in speech recognition (Chen et al., 2006; Hung-Yan Gu et al., 1991; Hieronymus et al., 1992; Oura et al., 2006), but also to classify human activities of daily living (Duong et al., 2005; Chung and Liu, 2008), handwriting (Kashi et al., 1997; Benouareth et al., 2007) and human genes in DNA (Kulp et al., 1996). HSMMs have also been used for language identification (Marcheret and Savic, 1997), the prediction of protein structure (Aydin et al., 2006), event recognition in videos (Hongeng and Nevatia, 2003), financial time series modelling (Bulla and Bulla, 2006), classification of music (XiaoBing Liu et al., 2008), and remote sensing (Pieczynski, 2007), among others.

Classical HMMs and HSMMs assume independence between the observations conditional on the state, but sometimes data is taken at high temporal resolution making this assumption unrealistic which can affect the performance of the classifiers. In such cases, autoregressive structure can be considered to model the observations of each state, leading to autorregressive HMMs and HSMMs (AR(p)-HMM and AR(p)-HSMM) (Xu and Liu, 2020), also commonly known as Markov-switching models. Even though these models have been extensively studied, as far as we are aware, these HMM extensions have not been used to classify acceleration data into animal behaviours.

In this paper, we give an overview of HMM, HSMM, AR(p)-HMM and AR(p)-HSMM; we explain the structure of these models in the supervised classification context, how they can be relaxed and their differences in modelling, inference, estimation, and prediction. We present their formulations and derivations as a compilation of the literature published on this topic. We then study how these models perform classifications under different scenarios in order to characterize when it would be important to extend an HMM to an HSMM. Finally, we use them to classify accelerometer data from domestic Merino sheep (*Ovis aries*) to distinguish between four different behavioural states.

2 Models

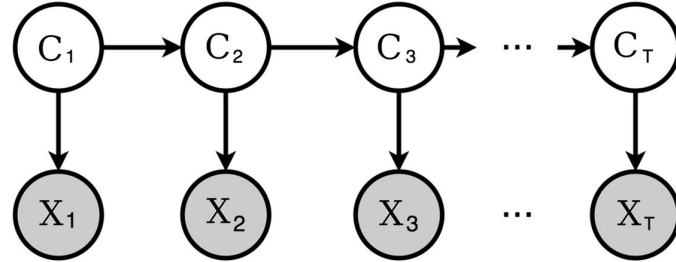
2.1 Hidden Markov Model (HMM)

HMMs are composed of two layers: a latent process $\{C_t\}_{t=1}^T$, commonly referred to as the state process, satisfying the Markov property; and an observable state-dependent process $\{X_t\}_{t=1}^T$, where $X_i \perp X_j | \mathbf{C}$ (Figure 1 (a)). At each point in time t , C_t is assumed to take on one of J possible values, $C_t \in \{1, 2, \dots, J\}$, where J denotes the number of states.

The dynamics of the state process \mathbf{C} are governed by a $J \times J$ transition probability matrix, $\mathbf{\Gamma}$, with entries $\gamma_{ij} = \Pr(C_{t+1} = j | C_t = i)$, for $i, j \in \{1, \dots, J\}$. The initial probabilities are denoted by $\delta_i = \Pr(C_1 = i)$, $i, j = 1, \dots, J$.

By definition, the assumption of a first-order Markov chain structure for the state process implies that the number of consecutive time points that the process spends in a given state before switching, i.e. the sojourn time, follows a geometric distribution with parameter γ_{ii} . As a consequence, the most likely sojourn time for every state of an HMM is one, and the probability of remaining in a given state decays geometrically. To complete the definition of an HMM, we denote the state-

(a) HMM



(b) HSMM

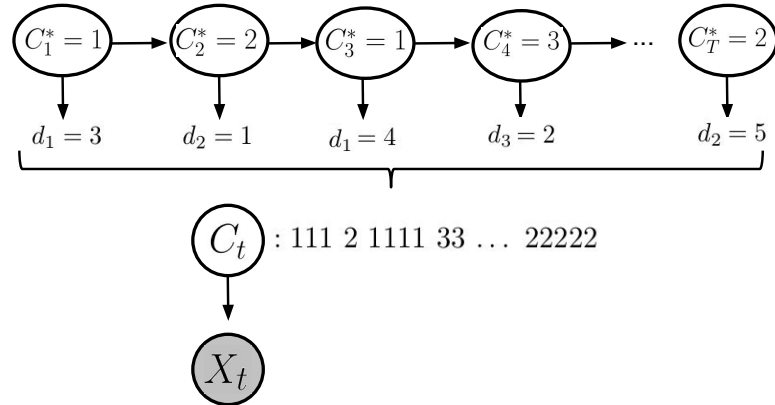


Figure 1: Diagrams of model structure (a)HMM : C_t denotes the latent Markov process and X_t denotes the observation process whose distribution depends on the state C_t . (b) HSMM example: C_t denotes the latent semi-Markov process and X_t the observation process. C_t^* indicates the Markovian process of the non absorbing times (that is, state at time t is equal to the state at time $t - 1$), and for each of them d_t gives the values of the sample sojourn times.

dependent distributions of the observation process (univariate or multivariate) as $f_j(x) = \Pr(X_t = x | C_t = j)$, for $j = 1, \dots, J$. The state-dependent distributions can be discrete or continuous and it is common to assume the same parametric distribution across all states. Therefore an HMM is defined by the pair of stochastic processes $\{X_t, C_t\}$, the state dependent distributions $f_1(x), \dots, f_J(x)$, the transition probability matrix Γ , and the initial probability vector $\boldsymbol{\delta} = (\delta_1, \dots, \delta_J)$.

2.2 Hidden Semi-Markov Model (HSMM)

One of the limitations of a basic HMM is the assumption that the sojourn time follows a geometric distribution. In fact, much work has been done to extend the basic HMM and explicitly model the sojourn time by other discrete-valued distributions, resulting in the class of hidden semi-Markov models (HSMM) (Yu, 2010). Like an HMM, an HSMM is a doubly stochastic process composed of two layers: a state process $\{C_t\}_{t=1}^T$ and an observable state-dependent process $\{X_t\}_{t=1}^T$. For an HSMM, however, the state process is now assumed to be a semi-Markov chain where the sojourn time in a given state is taken to follow any valid discrete distribution (e.g. Poisson, negative binomial). We provide definitions and notation of an HSMM in the remainder of the section.

In order to formalize the structure of the model, we first divide the times t into two disjoint categories depending on state C_t :

1. **Non absorbing time(NAT):** The state at time t is different than the state at time $t - 1$.

$$(C_t \neq C_{t-1})$$
2. **Absorbing time(AT):** The state at time t is equal to the state at time $t - 1$. $(C_t = C_{t-1})$.

The subsequence of states of non absorbing times is a first-order Markov process, while the sequence of C_t values is a finite-state semi-Markov chain. For simplicity, in this paper we assume that state switches occurred at time $t = 1$ and $t = T$, such that $C_1 \neq C_0$ and $C_T \neq C_{T+1}$. A HSMM with that simplifying assumption is called a right censored HSMM (Guédon, 2003).

For each state i of the non absorbing times, the sojourn time is a realization of the corresponding sojourn-time distribution d_i . Suppose that t^* is a non absorbing time of state i then $d_i(u) = \Pr(C_{t^*+u+1} \neq i \wedge C_{t^*+v} = i, v = 1, \dots, u | C_{t^*} = i)$, $u \geq 1$. For an HSMM, the t.p.m contains the conditional transition probabilities $(\Gamma)_{ij} = \gamma_{ij} = \Pr(C_{t+1} = j | C_t = i, C_{t+1} \neq i)$ $i \neq j$, $j = 1, \dots, J$ with $\gamma_{ii} = 0$ $\forall i = 1, \dots, J$. The probabilities of self-transitions are determined by d_i -sojourn distributions.

In Figure 1(b) an example of a 3-state HSMM ($C_t \in \{1, 2, 3\}$) is represented. The Markovian layer C_t^* governs the change of states and gives rise to a run of d values all equal to C_t^* . These d values are realizations from the sojourn time distributions d_i ($i = 1, 2, 3$). In this example $C_1^* = 1$ and $d_1 = 3$, indicating that the semi-Markov process starts with three ones, i.e. $C_1 = 1, C_2 = 1$ and $C_3 = 1$. Then $C_2^* = 2$ and $d_2 = 1$, indicating that the sequence follows with a single 2, $C_4 = 2$. Next $C_3^* = 1$ and $d_1 = 4$, so four ones are added to the sequence, $C_5 = 1, C_6 = 1, C_7 = 1, C_8 = 1$ and so on. The observation process is akin to an HMM in that the observations X_t are random variables that depend on the values of C_t . Therefore a HSMM can be defined by the pair of stochastic process $\{X_t, C_t\}$, X_t dependent on a semi-Markov chain C_t , the state dependent distributions $f_1(x), \dots, f_J(x)$, the sojourn-time distributions $d_1(u), \dots, d_J(u)$, the t.p.m Γ , and the initial state distribution $\delta = (\delta_1, \dots, \delta_J)$.

For the remainder of this article, we use the following notation. The observed sequence of length l , $(X_t, X_{t+1}, \dots, X_{t+l})$ is denoted by $\mathbf{X}_{t:t+l}$, and the state sequence $(C_t, C_{t+1}, \dots, C_{t+l})$ is denoted by $\mathbf{C}_{t:t+l}$. We use $\mathbf{C}_{[t_1:t_2]} = i$ to denote that the vector of state variables $\{C_{t_1} = i, C_{t_1+1} = i, \dots, C_{t_2} = i\}$ takes on the value i with state changes occurring at t_1 and $t_2 + 1$, $C_{t_1-1} \neq i$ and $C_{t_2+1} \neq i$. We let $\mathbf{C}_{[t_1:t_2]} = i$ denote similarly that the sequence of state variables $\{C_{t_1} = i, \dots, C_{t_2} = i\}$ take on the value i with a state change occurring at time t_1 , i.e. $C_{t_1-1} \neq i$, but allow for $C_{t_2+1} \in \{1, \dots, J\}$. Similarly $\mathbf{C}_{t_1:t_2]} = i$ denotes a state change at time $t_2 + 1$ but allows for $C_{t_1-1} \in \{1, \dots, J\}$. By $C_{[t_1]=i}$ we mean that at time t_1 the system switched from some other state to i , and by $C_{t_1]=i}$ that at time t_1 the state will end and transit to some other state. Finally, we let $\boldsymbol{\theta} = (\boldsymbol{\theta}_\delta, \boldsymbol{\theta}_P, \boldsymbol{\theta}_\Gamma, \boldsymbol{\theta}_d)$ be the vector of parameters of the HSMM: $\boldsymbol{\theta}_\delta$ the initial probabilities, $\boldsymbol{\theta}_P$ the parameters of the state dependence distributions $f_i(x)$, $\boldsymbol{\theta}_\Gamma$ the conditional transition probabilities of the t.p.m, and $\boldsymbol{\theta}_d$ the parameters of the sojourn time distributions $d_i(u)$.

2.3 Autoregressive Structure (AR(p)-HMM and AR(p)-HSMM)

In basic HMMs and HSMMs, we assume conditional independence of \mathbf{X} given \mathbf{C} . However, for time series collected at fine temporal scales, the autocorrelation structure may not adequately be captured using this framework. A common extension is to assume that the state-dependent distribution of $\{X_t\}_{t=2}^T$ depends on the current state C_t as well as on a subset of previous observations. This new assumption leads to an important class of models called Markov-switching models or autoregressive hidden (semi-)Markov models (Hamilton, 1994). In this framework, given the cur-

rent state, $\{X_t\}$ is assumed to follow state-dependent Gaussian autoregressive processes of order p (AR(p)):

$$x_t = \mu_i + \sum_{k=1}^p \omega_{ki} x_{t-k} + \epsilon_{ti} \quad \text{with } \epsilon_{ti} \sim N(0, \Sigma_i)$$

where μ_i , ω_{ki} and Σ_i are the conditional mean, autoregressive parameters and covariance matrix conditioned on $C_t = i$. We denote the state-dependant distributions of an AR(p)-HSMM as

$$f_i(x_t) = f(x_t | C_t = i, \mathbf{x}_{t-p:t-1})$$

and the joint distribution for vector $\mathbf{x}_{t:t'}$ with $t < t'$ as,

$$f_i(\mathbf{x}_{t:t'}) = \prod_{k=t}^{t'} f(x_k | C_k = i, \mathbf{x}_{k-p:k-1}) = \prod_{k=t}^{t'} f_i(x_k).$$

The use and statistical properties of HMMs with autoregresive structure have been studied and formalized (Yang, 2000; Francq and Zakoian, 2001), and further generalized for HSMMs Xu and Liu (2020). AR(p)-HSMM have been also used to perform classification in unsupervised manner; (Bryan and Levinson, 2015) demonstrates its application to speech signal recognition and (Duong et al., 2005) proposed the use of switching hidden semi-Markov model to recognize human activities of daily living. However, to our knowledge, the use of AR(p)-HSMM to perform supervised classification has not been studied or applied.

3 Classification via Supervised Learning

In many applications, the primary objective of the analysis is to accurately predict the latent states of the system. The observations themselves are not of real interest as their function is merely to provide information about the states (Zucchini et al., 2017). For processes that evolve over time (or in sequence), HMMs (and their extensions) can be applied to classify observations into different latent states while taking into account that observations *close to one another* in time are likely to have arisen from the same state. In this section we discuss the implementation of HMMs, HSMMs, and their respective autoregressive versions, in a supervised learning approach.

Supervised learning methods assume that there is a data set for which labels are available for all samples. This labeled data set is used to fit the model and asses its predictive capability. Then, the labelled data set is distributed among the train set to fit the model, the validation set to evaluate

the fitted model while tuning hyperparameters, and the test set to measure the accuracy of the final model. When there are not hyperparameters in the model, or these have already been fixed, the validation set is not necessary. Finally, once the model has been evaluated, it can be used to classify unlabelled data. Thus, when the aim is to perform classification using HMMs or HSMMs with a supervised approach, the steps are: split the labeled data, train the model (section 3.1), predict hidden states (section 3.2), estimate the classification error (section 3.3), and eventually classify unlabelled data.

3.1 Inference

Inference for $\boldsymbol{\theta}$ is done via use of the complete-data likelihood as both the observations and values of the states are known in the training data. The complete-data likelihood is expressed as the joint distribution of the observations, X_t , and states, C_t ,

$$\begin{aligned} f(\mathbf{c}_{1:T}, \mathbf{x}_{1:T} | \boldsymbol{\theta}) &= \Pr(\mathbf{C}_{1:T} = \mathbf{c}_{1:T}, \mathbf{X}_{1:T} = \mathbf{x}_{1:T} | \boldsymbol{\theta}) \\ &= \delta_{C_1} d_{C_1}(u_1) \prod_{t=1}^T f_{C_t}(x_t) \prod_{r \text{ is NAT}} \gamma_{c_{r-1}, c_r} d_{C_r}(u_r) \end{aligned}$$

Note that for the autoregressive case $f_{C_t}(x_t)$ depends on the p previous observations, i.e. $f_{C_t}(x_t) = f_{C_t}(x_t | \mathbf{x}_{t-p:t-1})$. The complete-data likelihood of an HMM necessarily has $d_{C_r}(\cdot) \sim \text{Geom}(\lambda_r)$.

The complete-data likelihood can be expressed as a product of the terms of the t.p.m., initial distribution, state-dependent distributions and sojourn time distributions, which allows the complete-data log-likelihood to be written as a sum,

$$\log(f(\mathbf{c}_{1:T}, \mathbf{x}_{1:T}, \boldsymbol{\theta})) = \log(\delta_{C_1}) + \log(d_{C_1}(u_1)) + \sum_{t=1}^T \log(f_{C_t}(x_t)) + \sum_{r \in \text{NAT}} \log(\gamma_{c_{r-1}, c_r}) + \log(d_{C_r}(u_r))$$

For K independent time series, the complete-data likelihood is the product of the individual complete-data likelihoods. As we conduct inference in a Bayesian framework, we first specify prior distributions for all parameters $f(\boldsymbol{\theta})$ and derive the joint posterior distribution $f(\boldsymbol{\theta} | \mathbf{x}_{1:T}, \mathbf{C}_{1:T}) \propto f(\mathbf{c}_{1:T}, \mathbf{x}_{1:T}, \boldsymbol{\theta}) f(\boldsymbol{\theta})$. In particular, the joint log posterior distribution can be expressed as a sum of the components of the complete-data log likelihood and prior distributions. Full details of the

prior distributions specified and derivation of the joint posterior distribution are provided in the Appendix (S1).

3.2 State prediction

The objective of classification, in this context, is to determine which states are likely to have generated the observations. This process is known as *state decoding* and can be done in one of two general ways: (i) *local state decoding* – identify the most likely state at each point in time or (ii) *global state decoding* – identify the sequence of states that is most likely to have generated the observation sequence. In what follows we formalize and discuss the most common algorithms and their adaptations to HSMMs and AR-HSMMs for state decoding.

3.2.1 Local State Decoding

Local state decoding is the process of determining at time t , what label of the state C_t is most likely to have generated the observation x_t . To do so, we compute and use the marginal probabilities $\Pr(C_t = i | \mathbf{X}_{1:T})$ via use of the forward-backward algorithm, which can be expressed as a function of the *so-called* forward probabilities $\{\alpha_t\}_{t=1}^T$ and backward probabilities $\{\beta_t\}_{t=1}^T$. For the basic HMM, these quantities are given as

$$\alpha_t(j) = \Pr(\mathbf{X}_{1:t}, C_t = j) \quad \beta_t(j) = \Pr(\mathbf{X}_{t+1:T} | C_t = j)$$

where $\beta_T(j) = 1$, for all $j \in \{1, \dots, J\}$ so that

$$\alpha_t(j) = f_j(x_t) \sum_i \gamma_{i,j} \alpha_{t-1}(i) \quad \beta_t(j) = \sum_i \beta_{t+1}(i) \gamma_{i,j} f_i(x_{t+1})$$

Given $\alpha_t(j)$ and $\beta_t(j)$, we can express the marginal probability as,

$$\Pr(C_t = j | \mathbf{X}_{1:T}) = \frac{\alpha_t(j) \beta_t(j)}{\Pr(\mathbf{X}_{1:T})}.$$

Further details are given in (Bishop, 2012; Zucchini et al., 2017). Derivation of the marginal state probabilities for the HSMM are similar to the HMM, while further adaptations are considered for the AR(p)-HSMM. We first express the forward and backwards probabilities as follows:

$$\alpha_t(j) = \Pr(\mathbf{X}_{1:t}, C_t = j) \quad \beta_t(j) = \Pr(\mathbf{X}_{t+1:T} | C_t = j, \mathbf{X}_{t-p:t})$$

It is also possible to give recurrence equations that express $\alpha_t(\cdot)$ in terms of $\alpha_{t-d}(\cdot)$ and $\beta_t(\cdot)$ in terms of $\beta_{t+d}(\cdot)$. For $t = 2, \dots, T$ and $j = 1, \dots, J$ it can be shown that,

$$\begin{aligned}\alpha_t(j) &= \sum_{d \in \mathcal{D}} \sum_{i \neq j} \alpha_{t-d}(i) \gamma_{ij} d_j(d) f_j(\mathbf{x}_{t-d+1:t}) \\ \beta_t(j) &= \sum_{d \in \mathcal{D}} \sum_{i \neq j} \beta_{t+d}(i) \gamma_{ji} d_i(d) f_i(\mathbf{x}_{t+1:t+d})\end{aligned}$$

Full details provided in Appendix S2.1. Let the marginal probabilities be expressed as $\xi_t(j) = \Pr(C_t = j, \mathbf{X}_{1:T})$ and let $\beta_t^*(j) = \Pr(\mathbf{X}_{t+1:T} | C_{[t+1]} = j)$ (or $\beta_t^*(j) = \Pr(\mathbf{X}_{t+1:T} | C_{[t+1]} = j, \mathbf{X}_{t-p:t})$ for the AR(p)-HSMM case). It follows from the definition of $\beta_t^*(j)$ that,

$$\begin{aligned}\beta_t(j) &= \sum_{i \neq j} \gamma_{ji} \beta_t^*(j) \\ \beta_t^*(j) &= \sum_{d \in \mathcal{D}} d_j(d) \beta_{t+d}(j) f_j(\mathbf{x}_{t+1:t+d})\end{aligned}$$

We can then calculate the marginal probabilities as follows (full details provided in the Appendix S2.1). For $t = 2, \dots, T$ and $j = 1, \dots, J$

$$\xi_t(j) = \xi_{t+1}(j) + \alpha_t(j) \sum_{i \neq j} \gamma_{ji} \beta_t^*(i) - \beta_t^*(j) \sum_{i \neq j} \alpha_t(i) \gamma_{ij}$$

For local state assignment, we use $\hat{C}_t = \arg \max_{j \in 1, \dots, J} \{\xi_t(j)\}$.

3.2.2 Global State Decoding

Global state decoding is a manner to identify the most likely sequence of states that could have given rise to the observed time series data. For this task, we determine the sequence c_1, c_2, \dots, c_T that maximizes the conditional probability $\Pr(\mathbf{C}_{1:T} | \mathbf{X}_{1:T})$ or equivalently the joint probability $\Pr(\mathbf{C}_{1:T}, \mathbf{X}_{1:T})$ via use of the Viterbi algorithm (Viterbi, 1967). For the basic HMM we first define

$$\psi_{1i} = \Pr(C_1 = i, X_1) = \delta_i f_i(x_1)$$

and for $t = 2, \dots, T$,

$$\psi_{ti} = \max_{c_{1:t-1}} \Pr(\mathbf{C}_{1:t-1}, C_t = i, \mathbf{X}_{1:t})$$

Given the following recursion,

$$\psi_{tj} = \left(\max_i (\psi_{t-1,i} \gamma_{ij}) \right) f_j(x_t) \quad (1)$$

the most probable state sequence is obtained by

$$\hat{i}_T = \operatorname{argmax}_{i=1,\dots,m} \psi_{Ti}$$

and for $t = T-1, T-2, \dots, 1$

$$\hat{i}_t = \operatorname{argmax}_{i=1,\dots,m} (\psi_{ti} \gamma_{i,i_{t+1}})$$

Global state decoding for an HSMM is similar to that of a basic HMM, but also requires that most likely sojourn times be determined in addition to the most likely state sequence. We define

$$\psi_t(j, d) = \max_{c_{1:t-d}} \Pr(\mathbf{C}_{1:t-d}, \mathbf{C}_{[t-d+1:t]}=j, \mathbf{X}_{1:T})$$

Similar to the basic HMM, it is possible to obtain the following recursion (full details provided in Appendix S2.2). For $t = 2, \dots, T$, $d = 1, \dots, D$ and $j = 1, \dots, J$

$$\psi_t(j, d) = \max_{\substack{i \neq j \\ d' \leq t}} \{ \psi_{t-d}(i, d') \gamma_{ij} d_j(d) f_j(\mathbf{x}_{t-d+1:t}) \}$$

Then, starting at time T , the most likely sequence of states and duration times is determined by

$$(\hat{i}_T, \hat{d}_T) = \operatorname{argmax}_{\substack{j=1,\dots,J \\ d=1,\dots,D}} \psi_T(j, d)$$

and for $t = T-1, \dots, 1$

$$(\hat{i}_t, \hat{d}_t) = \operatorname{argmax}_{\substack{j \neq \hat{i}_{t+1} \\ d=1,\dots,D}} \left(\psi_{t-d}(j, d') \gamma_{j, \hat{i}_{t+1}} d_{\hat{i}_{t+1}}(d) f_{\hat{i}_{t+1}}(\mathbf{x}_{t-d+1:t}) \right)$$

The results of local and global state decoding are often very similar but not identical (Zucchini et al., 2017). One advantage of local state decoding via the forward-backward algorithm over global state decoding via the Viterbi algorithm is that it provides an estimated probability for every possible state in all times. These probabilities provide information about the uncertainty over the predictions which can be useful for model comparison.

3.3 Classification Error

Given a fitted model, we can assess its capacity to classify the states correctly via both local and global state decoding. One of the most common measures to estimate prediction accuracy is the following classification accuracy index: the number of correct state predictions divided by the total number of observations in the time series. We can compute this measure from both the local and global decoding output. However, although this manner of estimating the prediction accuracy gives a general measure of the performance of the model, it does not take into account the uncertainty over the classification. Another manner to assess prediction capacity of our models is to use cross-entropy as it makes use of predicted probabilities of the states obtained via local state decoding and is given as,

$$CE = - \sum_{c=1}^J y_{x,c} \log(p_{x,c})$$

where $y_{x,c}$ is a binary indicator of whether state label c is the correct classification for observation x ($y_{x,c} = 1$ when the classification is correct), and $p_{x,c}$ is the predicted probability observation that x is generated by state c . The cross-entropy index increases as the predicted probability diverges from the actual label, such that a perfect model would have a CE value of 0.

To measure out-of-sample prediction accuracy (or error), we adapt *leave-one-out* cross validation to our application and use a *leave-one time series-out* cross-validation approach (Geisser, 1975; Refaeilzadeh et al., 2009). By doing so, we make the assumption that each time series is independent of each other and fulfill the requirement that the training and test sets are independent in order for CV approaches to be valid.

4 Simulation Study

In some applications the assumption that the sojourn times follow geometric distributions (HMMs) is far from being realistic. In such cases, HSMMs may be considered more appropriate as they allow that each state has variable duration time (Yu, 2010). However, when the main goal is to conduct classification it may not be necessary to extend the model to obtain correct state predictions. In this study we aim to characterize in which scenarios the state predictions of an HMM strongly differ from those of an HSMM, in order to understand when violating the assumption of geometric sojourn times can affect the accuracy of classifications.

We simulate different scenarios of univariate time series of length 3000 from a 2-state HSMM

with different sojourn times and observation distributions. Across all cases we assumed Gaussian distributions for the observations and negative binomial distributions for the sojourn times. We proposed three scenarios differing on the overlap between the observation distributions: the first assumes that $f_1(x_t) \sim N(0, 1)$ and $f_2(x_t) \sim N(0.3, 1)$ (high overlap), the second one assumes that $f_1(x_t) \sim N(0, 1)$ and $f_2(x_t) \sim N(1, 1)$ (medium overlap) and the last one assumes that $f_1(x_t) \sim N(0, 1)$ and $f_2(x_t) \sim N(3, 1)$ (low overlap). For each scenario we fixed different parameter values for the negative binomial distributions: $d_1 \sim NB(m_1, k_1)$ and $d_2 \sim NB(m_2, k_2)$, where m_1 and m_2 are the means and k_1 and k_2 the dispersion parameters. When $k = 1$ the negative binomial is a geometric distribution with probability $1/(m + 1)$, and as k takes values greater than 1 the dispersion of the distribution increases, moving away from the geometric distribution. In order to characterize different scenarios, we first set an average and a difference between m_1 and m_2 ($(m_1 + m_2)/2$ and $m_1 - m_2$). We considered as average between m_1 and m_2 : 90, 40 and 20, and as difference between them: 3, 15 and 30. We then varied k_1 and k_2 so that either k_1 equals 1 (one is geometric: $k_1 = 1$ and $k_2 = 10$ or $k_2 = 30$) or both k_1 and k_2 are greater than one (none are geometric: $k_1 = 30$ and $k_2 = 50$ or $k_1 = 80$ and $k_2 = 100$). For each parameter combination, we simulated ten time series of length 3000. To assess and compare the classification accuracy under both models (HMM and HSMM) we used *leave-one time series-out* cross-validation approach as follows: we fit both models with all the simulated time series but one, then sampling from the joint posterior distribution obtained, we predicted 30 times the hidden states of the simulated time series that we left out using Viterbi and FB algorithms. Finally we calculated the accuracy index of both predictions and the cross entropy value from the local decoding output. To perform the analysis we used R (R Core Team, 2019), to conduct parameter estimation we used Stan (Carpenter et al., 2017) and to implement the Viterbi algorithm for the HSMM we used the “hsmm.viterbi” function of the R package “hsmm” (<https://cran.r-project.org/web/packages/hsmm/index.html>).

Figure 2 shows the estimated accuracy values and the cross entropy index for each scenario obtained from the simulation analysis. It is clear that the performance of the models is lower when the overlap between the observations is larger: the cross entropy values increase and the accuracy indices decrease. When the average between m_1 and m_2 (the means of the sojourn time distributions) is large the differences between the three classification indices are low. However, when this average decreases the HSMM outperforms the HMM, since lower values of cross entropy index and higher values of accuracy are obtained. In general, for both models, the three indices improve as the average between m_1 and m_2 increases. With regards to the values of the dispersion parameters

(k_1 and k_2) of the sojourn times, it is clear that when one of the distributions is geometric (case 1 in the axis label), the differences between the models are smaller. This last fact makes sense with the model hypothesis, i.e. in HMMs the sojourn times follow a geometric distribution and in the HSMM they follow a negative binomial distribution.

The accuracy values of the FB algorithm and the Viterbi algorithm resulted to be practically equal in all the cases except when there is high overlap between the observation distributions and the average between m_1 and m_2 is low. In that case the accuracy values for the HSMM present higher dispersion: interquartile range between 0.05 and 0.55 for the HSMM, and 0.04 and 0.004 for the HMM. For the majority of the scenarios in terms of classification capacity the HSMM outperformed the HMM, obtaining larger differences when the overlap of the observation distributions increase, the average between the mean parameters of the sojourn times distributions decrease, and when the dispersion parameters are grater than one. Only when the overlap between the observation distributions is low and the averages between m_1 and m_2 are not too small, both models behave practically equally.

5 Sheep acceleration Data

We aim to classify accelerometer data from domestic merino sheep to distinguish between four different behavioural states. As animal accelerometer data is typically collected at a fine temporal resolution, leading to high temporal dependence of the observation process, we proposed the use of HMMs and HSMMs to classify the states. Fieldwork was conducted in Bariloche, Patagonia Argentina. The data used was collected from 25 different sheep during September and December of 2019. The animals were equipped with collars containing a DailyDiary(Wilson et al., 2008) developed at Swansea University, which were programmed to record 40 acceleration data per second (frequency of 40 Hz) and 13 magnetometer data per second (frequency of 13 Hz). The units recorded acceleration in three axes: anterior-posterior (surge), lateral (sway) and dorso-ventral (heave).

In order to obtain the labeled data set, recording sessions were done on September 24th, 2019, and December 17th, 2019. These recordings served as the groundtruthing for our behaviour recognition scheme. The acceleration data obtained was smoothed considering the moving average of windows of ten observations (a quarter of a second). From the observed data we distinguished four behaviours: (i) Inactive (when the animal is still: resting or vigilant), (ii) Walk (normal walking speed with the head raised), (iii) Fast Walk (when the animal runs or moves fast) and (iv) Foraging

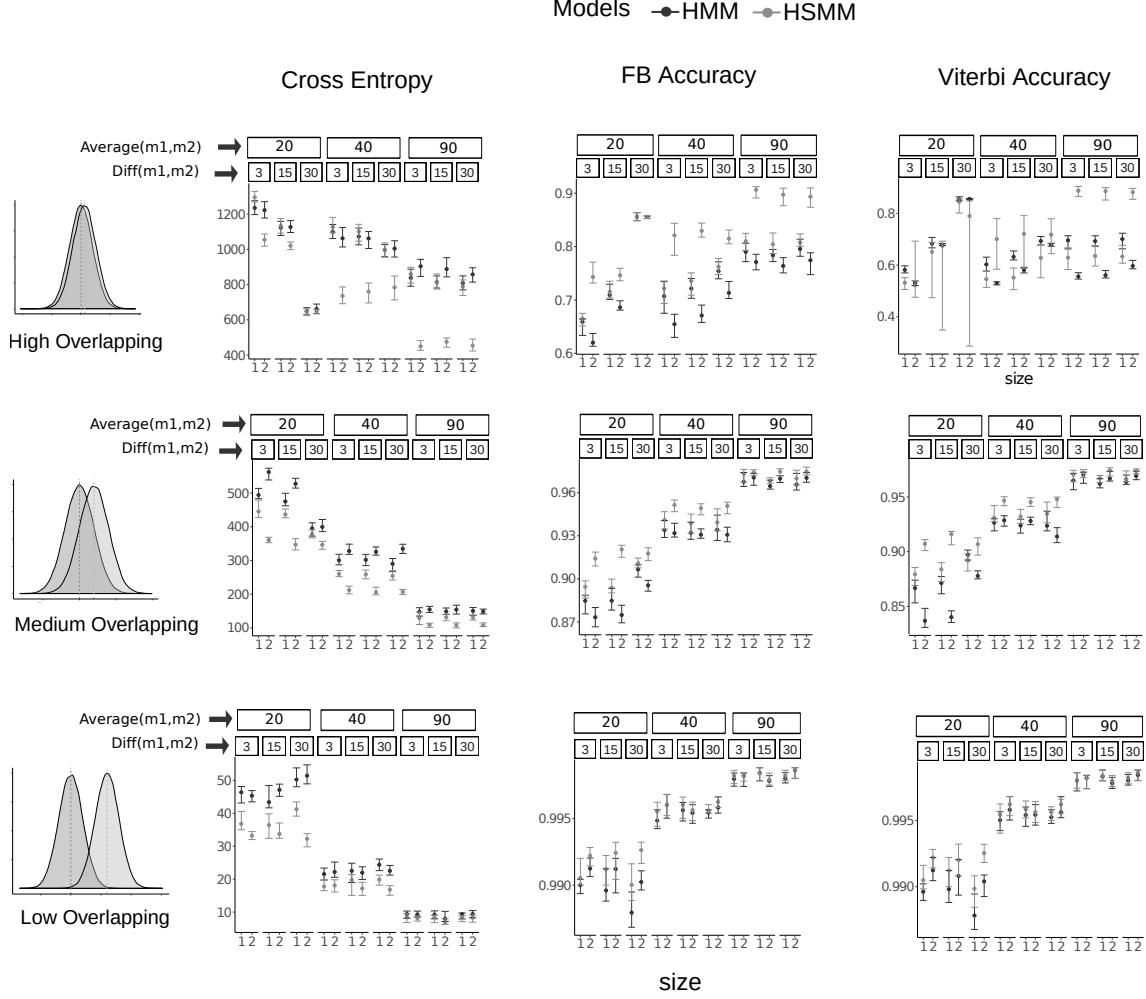


Figure 2: Values of the three indices computed for the simulation study. By column the index calculated (Cross Entropy, FB Accuracy and Viterbi Accuracy), by row the degree of overlap between the observation distributions (high, medium and low). In each box, the x-axis refers to the configuration of the dispersion parameters of the sojourn times (k_1 and k_2): for label 1 $k_1 = 1$ (one is geometric) and for label 2 neither k_1 nor k_2 equals 1 (none is geometric). Groups of three consecutive values of each box correspond to the different averages between m_1 and m_2 (20,40 and 90), and for each of them in order the three possible difference between m_1 and m_2 (3,15 and 30). Points represent the median value and bars depict the first and the third quartile. With black the values obtained for the HMMs and with gray the values obtained for the HSMMs.

(when the animal eats or looks for food. This can involve some walking but it is slow and with the head down). Manual classification was made at a 1s temporal resolution.

To define the variables involved in the observational process of the models, we identify the best characteristics that differentiate each behaviour, i.e. we determine acceleration-derived features with low overlapping distributions between the states. To accomplish that, we analyzed the acceleration axes and two derived values: the vectorial dynamic body acceleration(VeDBA, (Qasem et al., 2012)) and the head pitch angle (Wilson et al., 2008). The VeDBA is the square root of the sum of the squares of the three acceleration axes; this quantity can be considered as a proxy of the animal energy expenditure (Qasem et al., 2012). The head pitch can be derived from an approximation of the running mean of the surge sensors and it is a proxy of the angle of the head. It is primarily used to determine if the animal's head is facing upwards, in a neutral position, or downwards.

In the case of the sheep, the head pitch gives important information. The head of the animal looking down (negative pitch values) indicates foraging or searching behaviour, the head in a neutral position (pitch values near zero) indicates that the sheep is probably in an inactive state, and finally a variable orientation of the head measured at a level of one or two seconds (high variance of the pitch values) implies that the the sheep could be running or walking. The VeDBA index also gives useful information: low VeDBA values indicates less activity (inactive behaviour) and high values indicates more activity (walk and fast walk behaviours). After analyzing several summary statistics derived from these quantities and seeking to differentiate as best as possible the pre-established behaviors, we selected three summary statistics over a one second window: `log(Mean.VeDBA)`, the logarithm of the mean VeDBA over one second; `Mean.Pitch`, the mean Pitch angle over one second; and the `log(Sd.Pitch)`, the logarithm of the standard deviation of the Pitch angle over one second.

To distinguish between the four behavioural states and considering a 1s temporal scale, we analyzed the classifications derived from four models: (i) HMM, (ii)AR(1)-HMM, (iii) HSMM and (iv)AR(1)-HSMM. The following assumptions were made:

- $\forall t = 1, \dots, T, C_t \in \{1, 2, 3, 4\}$, with 1 = Walk, 2 = Fast-Walk, 3 = Inactive and 4 = Foraging
- $\boldsymbol{\delta} = (\frac{1}{4}, \frac{1}{4}, \frac{1}{4}, \frac{1}{4})$
- $\forall t = 1, \dots, T, \mathbf{X}_t = (X_t^1, X_t^2, X_t^3)$ with, X_t^1 the `log(Mean.VeDBA)` , X_t^2 the `Mean.Pitch`, and X_t^3 the `log(Sd.Pitch)`

For the non autoregressive models (i-iii)

- For $i \in \{1, 2, 3, 4\}$ $P(\mathbf{X}_t | C_t = i) \sim N(\mu_i, \Sigma_i)$, with Σ_i a diagonal matrix.

For the autoregressive models (ii-iv)

- For $i \in \{1, 2, 3, 4\}$ $P(\mathbf{X}_t | C_t = i) \sim N(\alpha_i + \beta_i x_{t-1}, \Sigma_i)$, with Σ_i a diagonal matrix.

and for the both HSMMs (iii-iv)

- For $i \in \{1, 2, 3, 4\}$ $d_i \sim NB(m_i, k_i)$, where m_i is the mean and k_i the dispersion parameter.

In order to assess the classification performance of the four models described above and considering the times series from each video as independent, we conducted a similar *leave-one time series-out* cross-validation approach as detailed in the previous section. In this case we first fit the four models with all the time series but one, and then predicted the remaining time series with the two decoding algorithms 100 times (sampling 100 times from the joint posterior distributions). Finally we calculated the two accuracy indices and the cross entropy value.

Furthermore, we fit the four models with all the time series available to analyze the ability of them to capture the structure of the system. In order to measure predictive capacity we computed a root mean square error (RMSE) over the observations: for each observed time series and model, using a 100 sample of the previously fitted posterior, we computed 100 predictions (using the FB algorithm) of the hidden states and the observation process. We then calculated the RMSE between the predictions and observations. To evaluate the goodness of fit we finally compared the estimations of the sojourn times assuming geometric distributions (HMM and AR(1)-HMM) and as negative binomial distributions (HSMM and AR(1)-HSMM) with the empirical distributions obtained from the observed sojourn times.

After discarding the videos that had not captured sheep or those for which acceleration data was not available, a total of 18 videos from eight different animals were obtained from the session of September and a total of 49 videos from 17 different animals from the session of December. Out of 67 time series with a total duration of two hours and 53 minutes, a 62.27% were from the Inactive behaviour, a 33.51% from the Foraging state, a 3.75% corresponded to the Walk class, and the remaining 0.47% to the Fast Walk state.

Figure 3 shows two examples of the signal patterns obtained for the four behaviours. When the sheep is inactive, the `log(Sd.Pitch)` and the `log(Mean.VedBA)` are low, meaning that the orientation of the head is almost constant and the energy expenditure is very low. When the sheep is eating or searching, the VedBA values are higher and the pitch angle is lower. The patterns of

the Walk behaviour are similar to the previous one, however, the pitch angle values can be higher and less constant. The highest values of the standard deviation of the `log(Mean.Pitch)` and of the `log(Mean.VedBA)` are obtained when the sheep is running. It also can be noticed that the four behaviours have different duration times: the inactive state is the one that lasts the longest, followed by the Foraging state, then the Walk behaviour and finally the Fast Walk state.

Figure 4 displays the boxplots obtained considering all the labelled data available for each behaviour for the three variables considered. It can be observed that for the three variables the distributions are fairly different between the four states. Even though the values of `log(Mean.VedBA)` for the Walk and Foraging states are similar, for the Inactive behaviour are clearly lower and for the Fast Walk behaviour higher. In regards to the `Mean.Pitch`, the Fast Walk and Inactive behaviours show similar distributions, but for the Walk state the values of `Mean.Pitch` are lower and for the Foraging behaviour are even minor (with dispersion). Finally, in spite of the fact that the values of `log(Sd.Pitch)` present greater dispersion, they are well differentiated between the four classes.

Figure 5 shows the values of the three classification indices calculated for each model. In all cases the models behave in a similar way and predict correctly. However, the models with autoregressive structure (AR(1)-HMM and AR(1)-HSMM) show less dispersion in all indices, suggesting less uncertainty over the classifications. When comparing the performances of the FB algorithm and the Viterbi algorithm no significant differences can be appreciated in the values of the accuracy index, suggesting that global and local decoding perform similarly in terms of classifications.

The estimated RMSE values(given in Appendix S3) reveal that there are no important differences in the predictive capacity between the four models. The estimated RMSE behaves similarly across the three variables, except for the case of `Log(Mean.VeDBA)` for which the non autoregressive models (HMM and HSMM) show less uncertainty. However, when analyzing the goodness of fit of the hidden process, it is clear that the estimations of the sojourn times of the HMMs differ from the estimations of the HSMMs (Figure 6). The empirical distribution of the sojourn times for the Walk and the Fast Walk behaviours evidence that the most likely dwell time is different from one, indicating that modeling these times with a geometric distribution would not be appropriate. Although in the case of the Inactive and the Foraging behaviours this pattern is less clear, the estimations of the HSMMs provide better approximations of the observed process.

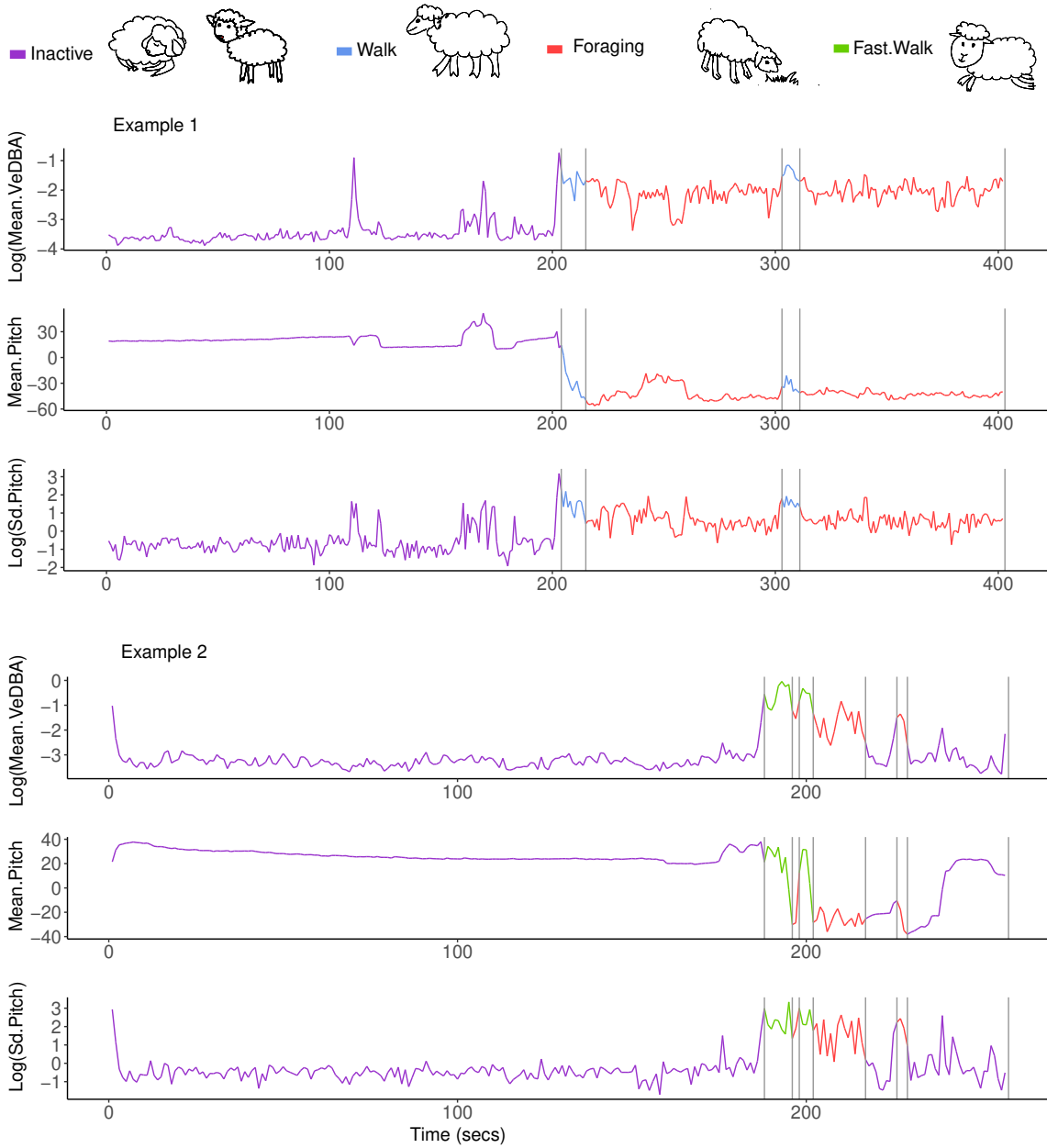


Figure 3: Two examples of the three features calculated from the acceleration signal logged from one sheep: $\text{log}(\text{Mean.VedBA})$, Mean.Pitch and $\text{log}(\text{Sd.Pitch})$. Different colors represent the signals corresponding to each of the four behaviors: Inactive (rest or vigilance), Walk, Foraging and Fast Walk.

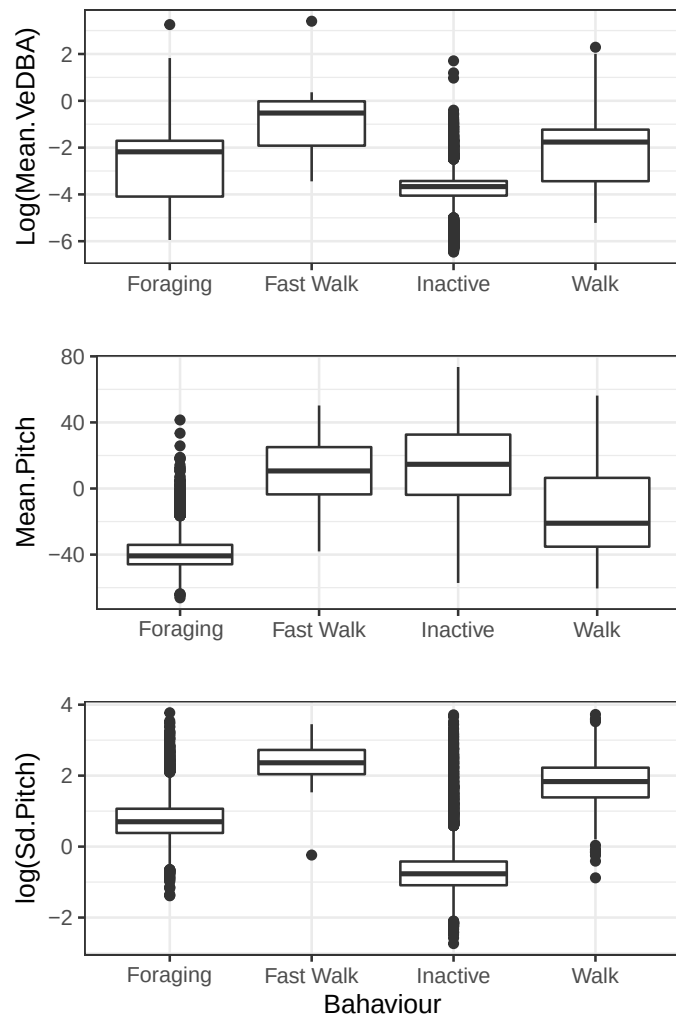


Figure 4: Boxplots of the $\text{log}(\text{Mean.VedBA})$, Mean.Pitch and $\text{log}(\text{Sd.Pitch})$ for each of the four behaviours: Inactive (rest or vigilance), Walk, Foraging and Fast Walk.

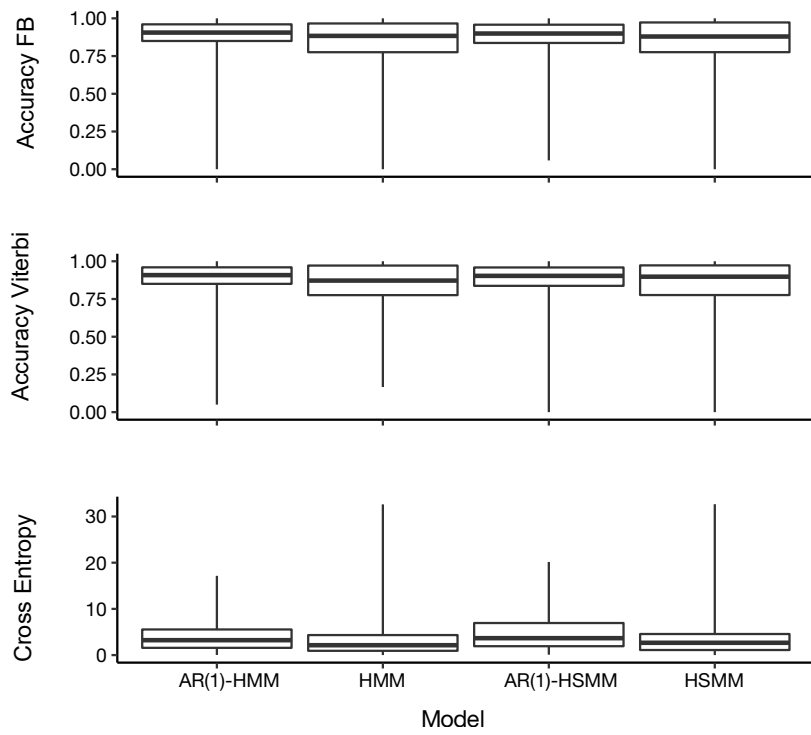


Figure 5: Boxplots of the accuracy values of both decoding algorithms and Cross Entropy index obtained by the LOOCV analysis for the four models considered: AR(1)-HMM, HMM, AR(1)-HSMM and HSMM.

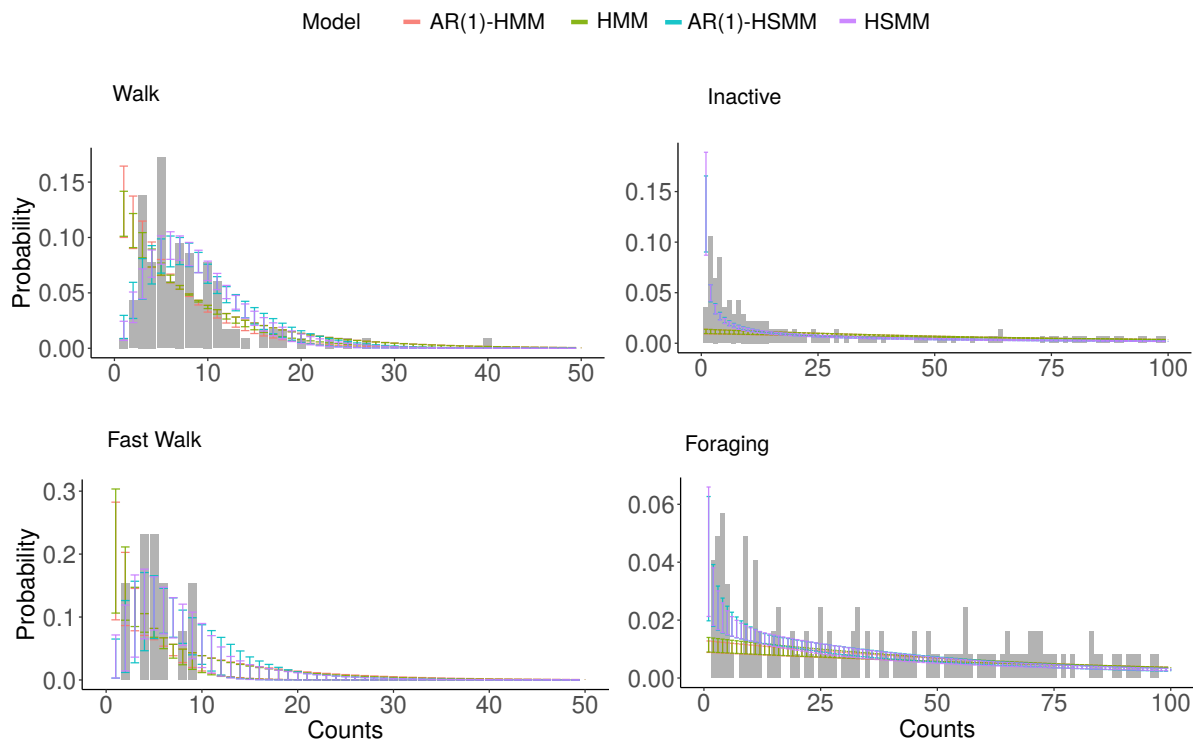


Figure 6: Fitted distributions of the sojourn times for each behaviour. The histogram displays the empirical distribution of the observed sojourn times while the four fitted models are displayed in color. The error bars indicate the pointwise estimates of the first and third quartile.

6 Discussion

We presented an overview of how to use HMMs and HSMMs with or without autoregressive structure in the observation process to perform supervised classification of time series data. We described how to extend an HMM to an HSMM, we detailed the model structures and presented the algorithms to predict the hidden states. We then studied cases under which the classifications from both models applied to time series data truly differ.

When the final aim is to conduct state classification, from the simulation study we can conclude that when the state-dependent distributions have high overlap and the sojourn times demonstrate that the most likely dwell time is different from one, unlike the geometric distribution, HSMMs outperform HMMs as the accuracy index is higher and the associated uncertainty is lower. However, when the overlap between the observation distributions is small or when the means of the sojourn time distributions greatly differ (regardless of their shape), the difference between models are minor.

We applied two HMMs and two HSMMs to sheep accelerometer data obtaining accurate predictions from all of them: in all cases we obtained values of accuracy index greater than 0.87 on average. Nonetheless, we could not see important differences between the performance of the four models as the error measures were similar. According to the simulation study results, this could be explained mainly due to the low overlap between the observation distributions, although the estimations of the sojourn time distributions were more consistent with the semi-Markovian approach. However, due to the manner in which the data was collected, it was not possible to obtain enough information to distinguish between vigilance and resting thus having to consider both as one behaviour (Inactive). The acceleration data from these two behaviours is practically identical, however the times that sheep spend in these two behaviours are vastly different: long rest times and much shorter vigilance times. We posit that if the data set could be more complete, extending the recording sessions in order to observe enough resting samples, different performance should be achieve between the four models.

When it comes to decide which model to use, the main consideration is the final goal of the analysis. When the aim is to conduct classification, the focus is on the ability to distinguish between different categories to then predict the unobserved states. However, if the aim is to also provide a mechanism for data generation, the robustness of the model hypotheses becomes relevant. In those cases, correct specifications and accurate estimations should be taken into account to achieve the objectives of the analysis.

When the aim is to select a model with good classification performance, various degrees of model misspecification may not result in state predictions that differ greatly from those obtained from the correctly specified model. If the state-dependent distributions greatly differ, simple models incorrectly specified can perform equally as well as those that are correctly specified. However, if there is a high overlap between the state distributions, correctly specified models will improve the performance of the analysis.

When the purpose is to classify observations from time series data, HMMs and HSMMs resulted to be appropriate as they explicitly include sequential correlation into the analysis. Due to the structure of these models, they allow to distinguish between the sequential dependence present in the data and the temporal structure of consecutive states. The difference between an HMM and an HSMM is that the latter allows for explicit duration modeling of the behavioral process. When there is significant overlap between the observation distributions and the sojourn times distributions do not have geometric form, considering extending the model to improve the model specifications should benefit the accuracy of the classifications. However, when the observation distributions are different between states and even more, if the sojourn time distributions also differ, even if the model fails in some assumptions, the classifications from an HMM can be as accurate as the classifications from an HSMM that is better specified.

References

Z. Aydin, Y. Altunbasak, and M. Borodovsky. Protein secondary structure prediction for a single-sequence using hidden semi-Markov models. *BMC Bioinformatics*, 7(1):178, 2006. ISSN 1471-2105. doi: 10.1186/1471-2105-7-178.

A. Benouareth, A. Ennaji, and M. Sellami. Arabic Handwritten Word Recognition Using HMMs with Explicit State Duration. *EURASIP Journal on Advances in Signal Processing*, 2008(1):247354, 2007. ISSN 1687-6180. doi: 10.1155/2008/247354.

C. M. Bishop. Model-based machine learning. *Philosophical Transactions of the Royal Society A: Mathematical, Physical and Engineering Sciences*, 371(1984):20120222–20120222, Dec. 2012. ISSN 1364-503X, 1471-2962. doi: 10.1098/rsta.2012.0222.

J. D. Bryan and S. E. Levinson. Autoregressive Hidden Markov Model and the Speech Signal. *Procedia Computer Science*, 61:328–333, 2015. ISSN 18770509. doi: 10.1016/j.procs.2015.09.151.

J. Bulla and I. Bulla. Stylized facts of financial time series and hidden semi-markov models. *Computational Statistics & Data Analysis*, 51(4):2192–2209, 2006. ISSN 0167-9473. doi: <https://doi.org/10.1016/j.csda.2006.07.021>.

B. Carpenter, A. Gelman, M. Hoffman, D. Lee, B. Goodrich, M. Betancourt, M. Brubaker, J. Guo, P. Li, and A. Riddell. Stan: A probabilistic programming language. *Journal of Statistical Software*, 76:1, 2017. doi: DOI10.18637/jss.v076.i01.

G. Carroll, D. Slip, I. Jonsen, and R. Harcourt. Supervised accelerometry analysis can identify prey capture by penguins at sea. *Journal of Experimental Biology*, 217(24):4295–4302, Dec. 2014. ISSN 0022-0949, 1477-9145. doi: 10.1242/jeb.113076.

P. Chakravarty, G. Cozzi, A. Ozgul, and K. Aminian. A novel biomechanical approach for animal behaviour recognition using accelerometers. *Methods in Ecology and Evolution*, 10(6):802–814, June 2019. ISSN 2041-210X, 2041-210X. doi: 10.1111/2041-210X.13172.

K. Chen, M. Hasegawa-Johnson, A. Cohen, S. Borys, Sung-Suk Kim, J. Cole, and Jeung-Yoon Choi. Prosody dependent speech recognition on radio news corpus of american english. *IEEE Transactions on Audio, Speech, and Language Processing*, 14(1):232–245, 2006. doi: 10.1109/TSA.2005.853208.

W. T. Cheng and K. L. Chan. Classification of electrocardiogram using hidden markov models. In *Proceedings of the 20th Annual International Conference of the IEEE Engineering in Medicine and Biology Society*. Vol.20 Biomedical Engineering Towards the Year 2000 and Beyond (Cat. No.98CH36286), pages 143–146 vol.1, 1998. doi: 10.1109/IEMBS.1998.745850.

P.-C. Chung and C.-D. Liu. A daily behavior enabled hidden markov model for human behavior understanding. *Pattern Recognition*, 41(5):1572–1580, 2008. ISSN 0031-3203. doi: <https://doi.org/10.1016/j.patcog.2007.10.022>.

L. Deng and X. Li. Machine learning paradigms for speech recognition: An overview. *IEEE Transactions on Audio, Speech, and Language Processing*, 21(5):1060–1089, 2013. doi: 10.1109/TASL.2013.2244083.

T. G. Dietterich. Machine Learning for Sequential Data: A Review. In T. Caelli, A. Amin, R. P. W. Duin, D. de Ridder, and M. Kamel, editors, *Structural, Syntactic, and Statistical*

Pattern Recognition, Lecture Notes in Computer Science, pages 15–30. Springer Berlin Heidelberg, 2002. ISBN 978-3-540-70659-5.

T. V. Duong, H. H. Bui, D. Q. Phung, and S. Venkatesh. Activity recognition and abnormality detection with the switching hidden semi-markov model. In *2005 IEEE Computer Society Conference on Computer Vision and Pattern Recognition (CVPR'05)*, volume 1, pages 838–845 vol. 1, June 2005. doi: 10.1109/CVPR.2005.61.

C. Francq and J.-M. Zakoian. Stationarity of multivariate Markov–switching ARMA models. *Journal of Econometrics*, 102(2):339–364, June 2001. ISSN 03044076. doi: 10.1016/S0304-4076(01)00057-4.

S. Frühwirth-Schnatter, G. Celeux, and C. P. Robert, editors. *Handbook of mixture analysis*. CRC Press, Taylor & Francis Group, Boca Raton, 2019. ISBN 978-1-4987-6381-3.

S. Geisser. The predictive sample reuse method with applications. *Journal of the American Statistical Association*, 70(350):320–328, 1975. doi: 10.1080/01621459.1975.10479865.

P. Geurts. Pattern extraction for time series classification. In L. De Raedt and A. Siebes, editors, *Principles of Data Mining and Knowledge Discovery*, pages 115–127, Berlin, Heidelberg, 2001. Springer Berlin Heidelberg.

Y. Guédon. Estimating hidden semi-Markov chains from discrete sequences. *Journal of Computational and Graphical Statistics*, 12(3):604–639, 2003. doi: 10.1198/1061860032030.

J. Hamilton. *Time Series Analysis*. Princeton University Press, Princeton, NJ, 1994.

J. L. Hieronymus, D. McKelvie, and F. R. McInnes. Use of acoustic sentence level and lexical stress in hsmm speech recognition. In *Proceedings of the 1992 IEEE International Conference on Acoustics, Speech and Signal Processing - Volume 1*, ICASSP'92, page 225–227, USA, 1992. IEEE Computer Society. ISBN 0780305329.

S. Hongeng and R. Nevatia. Large-scale event detection using semi-hidden markov models. In *Proceedings of the Ninth IEEE International Conference on Computer Vision - Volume 2*, ICCV '03, page 1455, USA, 2003. IEEE Computer Society. ISBN 0769519504.

Hung-Yan Gu, Chiu-Yu Tseng, and Lin-Shan Lee. Isolated-utterance speech recognition using hidden markov models with bounded state durations. *IEEE Transactions on Signal Processing*, 39(8):1743–1752, 1991. doi: 10.1109/78.91145.

O. T. Inan, L. Giovangrandi, and G. T. A. Kovacs. Robust neural-network-based classification of premature ventricular contractions using wavelet transform and timing interval features. *IEEE Transactions on Biomedical Engineering*, 53(12):2507–2515, 2006. doi: 10.1109/TBME.2006.880879.

I. Jonsen. Joint estimation over multiple individuals improves behavioural state inference from animal movement data. *Scientific Reports*, 6(1):20625, 2016. ISSN 2045-2322. doi: 10.1038/srep20625.

B. H. Juang and L. R. Rabiner. Hidden markov models for speech recognition. *Technometrics*, 33(3):251–272, 1991. doi: 10.1080/00401706.1991.10484833.

R. S. Kashi, J. Hu, W. L. Nelson, and W. Turin. On-line handwritten signature verification using hidden markov model features. In *Proceedings of the Fourth International Conference on Document Analysis and Recognition*, volume 1, pages 253–257 vol.1, 1997. doi: 10.1109/ICDAR.1997.619851.

D. Kulp, D. Haussler, M. G. Reese, and F. H. Eeckman. A generalized hidden Markov model for the recognition of human genes in DNA. *Proceedings. International Conference on Intelligent Systems for Molecular Biology*, 4:134–142, 1996. ISSN 1553-0833 (Print).

R. Langrock and W. Zucchini. Hidden markov models with arbitrary state dwell-time distributions. *Computational Statistics & Data Analysis*, 55(1):715–724, 2011. ISSN 0167-9473. doi: <https://doi.org/10.1016/j.csda.2010.06.015>.

V. Leos-Barajas, T. Photopoulou, R. Langrock, T. Patterson, Y. Watanabe, M. Murgatroyd, and Y. Papastamatiou. Analysis of animal accelerometer data using hidden Markov models. *Methods in Ecology and Evolution*, Feb. 2017. doi: 10.1111/2041-210X.12657.

A. Li, L. Ji, S. Wang, and J. Wu. Physical activity classification using a single triaxial accelerometer based on HMM. In *IET International Conference on Wireless Sensor Network 2010 (IET-WSN 2010)*, pages 155–160, Nov. 2010. doi: 10.1049/cp.2010.1045.

E. Marcheret and M. Savic. Random walk theory applied to language identification. In 1997 IEEE International Conference on Acoustics, Speech, and Signal Processing, volume 2, pages 1119–1122 vol.2, 1997. doi: 10.1109/ICASSP.1997.596138.

Mevin B. Hooten, Devin S. Johnson, Brett T. McClintock, and Juan M. Morales. Animal Movement: Statistical Models for Telemetry Data. CRC Press, 2017.

J. M. Morales, P. R. Moorcroft, J. Matthiopoulos, J. L. Frair, J. G. Kie, R. A. Powell, E. H. Merrill, and D. T. Haydon. Building the bridge between animal movement and population dynamics. Philosophical Transactions of the Royal Society of London B: Biological Sciences, 365(1550): 2289–2301, jul 2010. ISSN 0962-8436, 1471-2970. doi: 10.1098/rstb.2010.0082.

R. Nathan. PNAS-2008-Nathan-19050-1. Proceedings of the National Academy of Sciences, 105 (49):19050–19051, 2008.

R. Nathan, O. Spiegel, S. Fortmann-Roe, R. Harel, M. Wikelski, and W. M. Getz. Using tri-axial acceleration data to identify behavioral modes of free-ranging animals: general concepts and tools illustrated for griffon vultures. Journal of Experimental Biology, 215(6):986–996, Mar. 2012. ISSN 0022-0949, 1477-9145. doi: 10.1242/jeb.058602.

K. Oura, Heiga Zen, Y. Nankaku, Akinobu Lee, and K. Tokuda. Hidden semi-markov model based speech recognition system using weighted finite-state transducer. In 2006 IEEE International Conference on Acoustics Speech and Signal Processing Proceedings, volume 1, pages I–I, 2006. doi: 10.1109/ICASSP.2006.1659950.

W. Pieczynski. Multisensor triplet markov chains and theory of evidence. Int. J. Approx. Reasoning, 45(1):1–16, May 2007. ISSN 0888-613X. doi: 10.1016/j.ijar.2006.05.001.

L. Qasem, A. Cardew, A. Wilson, I. Griffiths, L. Halsey, E. Shepard, A. Gleiss, and R. Wilson. Tri-axial dynamic acceleration as a proxy for animal energy expenditure; should we be summing values or calculating the vector? PloS one, 7:e31187, 02 2012. doi: 10.1371/journal.pone.0031187.

R Core Team. R: A Language and Environment for Statistical Computing. R Foundation for Statistical Computing, Vienna, Austria, 2019. URL <https://www.R-project.org>.

P. Refaeilzadeh, L. Tang, and H. Liu. Cross-Validation, pages 532–538. Springer US, Boston, MA, 2009. ISBN 978-0-387-39940-9. doi: 10.1007/978-0-387-39940-9_565.

M. A. Rico-Ramirez and I. D. Cluckie. Classification of ground clutter and anomalous propagation using dual-polarization weather radar. *IEEE Transactions on Geoscience and Remote Sensing*, 46(7):1892–1904, 2008. doi: 10.1109/TGRS.2008.916979.

S. Ruiz-Suarez, M. Sued, L. Vidal, P. Salio, D. Rodriguez, S. Nesbitt, and Y. Garcia Skabar. Técnicas de clasificación supervisada para la discriminación entre ecos meteorológicos y no meteorológicos usando información de un radar de banda C. *Meteorológica*, 44:45–65, 2019.

E. K. Studd, M. Landry-Cuerrier, A. K. Menzies, S. Boutin, A. G. McAdam, J. E. Lane, and M. M. Humphries. Behavioral classification of low-frequency acceleration and temperature data from a free-ranging small mammal. *Ecology and Evolution*, 9(1):619–630, Jan. 2019. ISSN 2045-7758. doi: 10.1002/ece3.4786. Publisher: John Wiley & Sons, Ltd.

Trevor Hastie, Robert Tibshirani, and Jerome Friedman. *The Elements of Statistical Learning*. Springer, New York, NY, USA, 2001.

A. Viterbi. Error bounds for convolutional codes and an asymptotically optimum decoding algorithm. *IEEE Transactions on Information Theory*, 13(2):260–269, 1967. doi: 10.1109/TIT.1967.1054010.

J. Wang, R. Chen, X. Sun, M. F. H. She, and Y. Wu. Recognizing Human Daily Activities From Accelerometer Signal. *Procedia Engineering*, 15:1780–1786, Jan. 2011. ISSN 1877-7058. doi: 10.1016/j.proeng.2011.08.331.

H. J. Williams, E. L. C. Shepard, O. Duriez, and S. A. Lambertucci. Can accelerometry be used to distinguish between flight types in soaring birds? *Animal Biotelemetry*, 3(1), Dec. 2015. ISSN 2050-3385. doi: 10.1186/s40317-015-0077-0.

H. J. Williams, L. A. Taylor, S. Benhamou, A. I. Bijleveld, T. A. Clay, S. de Grissac, U. Demšar, H. M. English, N. Franconi, A. Gómez-Laich, R. C. Griffiths, W. P. Kay, J. M. Morales, J. R. Potts, K. F. Rogerson, C. Rutz, A. Spelt, A. M. Trevail, R. P. Wilson, and L. Börger. Optimizing the use of biologgers for movement ecology research. *Journal of Animal Ecology*, 89(1):186–206, 2020. doi: <https://doi.org/10.1111/1365-2656.13094>.

R. Wilson, E. Shepard, and N. Liebsch. Prying into the intimate details of animal lives: Use of a daily diary on animals. *Endangered Species Research*, 4:123–137, 01 2008. doi: 10.3354/esr00064.

XiaoBing Liu, DeShun Yang, and XiaoOu Chen. New approach to classification of chinese folk music based on extension of hmm. In 2008 International Conference on Audio, Language and Image Processing, pages 1172–1179, 2008. doi: 10.1109/ICALIP.2008.4590068.

Z. Xu and Y. Liu. A Regularized Vector Autoregressive Hidden Semi-Markov Model, with Application to Multivariate Financial Data. arXiv:1804.10308 [stat], Feb. 2020. arXiv: 1804.10308.

M. Yang. Some properties of vector autoregressive processes with Markov-switching coefficients. Econometric Theory, 16:23–43, Feb. 2000. doi: 10.1017/S026646660016102X.

S.-Z. Yu. Hidden semi-Markov models. Artificial Intelligence, 174(2):215–243, Feb. 2010. ISSN 00043702. doi: 10.1016/j.artint.2009.11.011.

W. Zucchini, I. L. MacDonald, and R. Langrock. Hidden Markov Models for Time Series: An Introduction Using R, Second Edition. CRC Press, Dec. 2017. ISBN 978-1-4822-5384-9.

1 Supporting Information

2

3 **1 Bayesian Inference**

4 To conduct classification via supervised learning, both the observations and values of the states are known
 5 from the training data. To fit the values of the model under the Bayesian approach, the posterior distributions
 6 of the parameters are computed. In section 3.1 of the main manuscript, we present the joint posterior
 7 distribution of the parameters as the product of the complete data likelihood and the prior distributions

$$f(\boldsymbol{\theta}|\mathbf{x}_{1:T}, \mathbf{c}_{1:T}) \propto f(\mathbf{c}_{1:T}, \mathbf{x}_{1:T}, \boldsymbol{\theta})f(\boldsymbol{\theta})$$

8 Let us distinguish the different elements of the parameter vector. Be $\boldsymbol{\theta} = (\boldsymbol{\delta}, \boldsymbol{\gamma}, \boldsymbol{\theta}_{obs}, \boldsymbol{\theta}_d)$, where $\boldsymbol{\delta}$ is the
 9 parameter vector of the initial distributions, $\boldsymbol{\gamma}$ the parameter vector of the transition probability matrix,
 10 $\boldsymbol{\theta}_{obs}$ the parameter vector of the observation distributions and $\boldsymbol{\theta}_d$ the vector parameter of the sojourn time
 11 distributions. If we consider independent priors

$$f(\boldsymbol{\theta}) = f(\boldsymbol{\delta})f(\boldsymbol{\gamma})f(\boldsymbol{\theta}_{obs})f(\boldsymbol{\theta}_d)$$

12 the posterior distribution can then be split into separate components

$$f(\boldsymbol{\theta}|\mathbf{x}_{1:T}, \mathbf{c}_{1:T}) = f(\boldsymbol{\delta}|\mathbf{x}_{1:T}, \mathbf{c}_{1:T})f(\boldsymbol{\gamma}|\mathbf{x}_{1:T}, \mathbf{c}_{1:T})f(\boldsymbol{\theta}_{obs}|\mathbf{x}_{1:T}, \mathbf{c}_{1:T})f(\boldsymbol{\theta}_d|\mathbf{x}_{1:T}, \mathbf{c}_{1:T})$$

13 In what follows we detail the formulation of each component

14 **Specifications for the transition and initial distributions**

15 If we consider $f(\boldsymbol{\gamma})$ to follow a Dirichlet distribution, i.e. $f(\boldsymbol{\gamma}) \sim \mathcal{D}(\kappa_{j1}, \dots, \kappa_{jJ})$ for $j = 1 \dots J$, as the
 16 changes of state have multinomial distribution, the posterior distribution for $\boldsymbol{\gamma}$ is also Dirichlet

$$f(\boldsymbol{\gamma}|\mathbf{x}_{1:T}, \mathbf{c}_{1:T}) \propto \mathcal{D}(\kappa_{j1} + \nu_{j1}, \dots, \kappa_{jJ} + \nu_{jJ})$$

17 with ν_{ji} = number of occurrences from state j to i . Similarly for $f(\delta | \mathbf{x}_{1:T}, \mathbf{c}_{1:T})$, consider $f(\delta) \sim \mathcal{D}(\omega_1, \dots, \omega_J)$,
 18 then

$$f(\delta | \mathbf{x}_{1:T}, \mathbf{c}_{1:T}) \propto \mathcal{D}(\omega_1 + \tau_1, \dots, \omega_J + \tau_J)$$

19 with τ_j = number of times an observed series begins with state j

20 Specifications for the observation distributions

21 Given J states, it is necessary to make inference about the parameters of J state-dependent distributions
 22 $f_1(x) \dots f_J(x)$. Each $j = 1 \dots J$ group of parameters, θ_{obs_j} , is estimated using only the observations allocated
 23 to state j . Then

$$f_j(\theta_{obs} | \mathbf{x}_{1:T}, \mathbf{c}_{1:T}) = f_j(\theta_{obs_j} | \mathbf{x}_{[j]})$$

24 where $\mathbf{x}_{[j]} = \{x_t / C_t = j\}$.

25 In this paper the state-dependent observations are assumed to be normally distributed

$$f_j(x) \sim N(\mu_j, \Sigma_j)$$

26 We consider independent Normal priors for the J observation distributions. $f(\theta_{obs_j}) = f(\mu_j) f(\Sigma_j)$
 27 $f(\mu_j) \sim N(\mu_{0j}, \Sigma_{0j})$ and $f(\Sigma_j) \sim NT(\mu_{0j}, \Sigma_{0j}, 0, \infty)$
 28 where NT indicates a truncated normal distribution. In this case, the posterior distributions do not have
 29 a closed form. They can be formulated as

$$f_j(\theta_{obs_j} | \mathbf{x}_{1:T}, \mathbf{c}_{1:T}) \propto f(\theta_{obs_j}) \prod_{t/C_t=j} f_j(x_t)$$

30 Specifications for the sojourn time distributions

31 Once again, it is necessary to make inference about the parameters of J state-dependent distributions
 32 $d_1(x) \dots d_J(x)$. Each $j = 1 \dots J$ group of parameters, θ_{d_j} , is estimated using only the dwell times of
 33 the observations allocated to state j .

34 As we consider negative binomial distributions for the J sojourn time distributions, the posterior distributions
 35 do not have a closed form. They can be formulated as

$$f_j(\boldsymbol{\theta}_{d_j} | \mathbf{x}_{1:T}, \mathbf{c}_{1:T}) \propto f(\boldsymbol{\theta}_{d_j}) \prod_{\substack{r \text{ is NAT} \\ \text{and } C_r=j}} d_{Cr}(u_r)$$

36 2 Proofs

37 In the following section some of the results used in the main manuscript are proven. With **blue** are marked
 38 the considerations for the autoregressive case.

39 2.1 From Local Decoding section

Proposition 1. For $t = 2, \dots, T$ and $j = 1, \dots, J$

$$\alpha_t(j) = \sum_{d \in \mathcal{D}} \sum_{i \neq j} \alpha_{t-d}(i) \gamma_{ij} d_j(d) f_j(\mathbf{x}_{t-d+1:t})$$

Proof.

$$\begin{aligned} \alpha_t(j) &= \Pr(C_t = j, \mathbf{X}_{1:t}) \\ &= \sum_{d \in \mathcal{D}} \Pr(\mathbf{C}_{[t-d+1:t]} = j, \mathbf{X}_{1:t}) \\ &= \sum_{d \in \mathcal{D}} \Pr(\mathbf{X}_{t-d+1:t} | \mathbf{X}_{1:t-d}, \mathbf{C}_{[t-d+1:t]} = j) \Pr(\mathbf{X}_{1:t-d}, \mathbf{C}_{[t-d+1:t]} = j) \\ &= \sum_{d \in \mathcal{D}} f_j(\mathbf{x}_{t-d+1:t}) \Pr(\mathbf{X}_{1:t-d}, \mathbf{C}_{[t-d+1:t]} = j) \end{aligned}$$

40 And we have

$$\begin{aligned} \Pr(\mathbf{X}_{1:t-d}, \mathbf{C}_{[t-d+1:t]} = j) &= \Pr(\mathbf{X}_{1:t-d} | \mathbf{C}_{[t-d+1:t]} = j) d_j(d) \\ &= \sum_{i \neq j} \Pr(\mathbf{X}_{1:t-d}, C_{t-d} = i | \mathbf{C}_{[t-d+1:t]} = j) d_j(d) \\ &= \sum_{i \neq j} \Pr(\mathbf{X}_{1:t-d}, C_{t-d} = i) \gamma_{ij} d_j(d) \\ &= \sum_{i \neq j} \alpha_{t-d}(i) \gamma_{ij} d_j(d) \end{aligned}$$

Proposition 2. For $t = 2, \dots, T$ and $j = 1, \dots, J$

$$\beta_t(j) = \sum_{d \in \mathcal{D}} \sum_{i \neq j} \beta_{t+d}(i) \gamma_{ji} d_i(d) f_i(\mathbf{x}_{t+1:t+d})$$

Proof.

$$\begin{aligned} \beta_t(j) &= \Pr(\mathbf{X}_{t+1:T} | C_t = j, \mathbf{X}_{t-\mathbf{p}:t}) \\ &= \sum_{d \in \mathcal{D}} \sum_{i \neq j} \Pr(\mathbf{X}_{t+1:T}, \mathbf{C}_{[t+1:t+d]} = i | C_t = j, \mathbf{X}_{t-\mathbf{p}:t}) \\ &= \sum_{d \in \mathcal{D}} \sum_{i \neq j} \Pr(\mathbf{X}_{t+1:T} | \mathbf{C}_{[t+1:t+d]} = i, C_t = j, \mathbf{X}_{t-\mathbf{p}:t}) \Pr(\mathbf{C}_{[t+1:t+d]} = i | C_t = j, \mathbf{X}_{t-\mathbf{p}:t}) \\ &= \sum_{d \in \mathcal{D}} \sum_{i \neq j} \Pr(\mathbf{X}_{t+1:t+d}, \mathbf{X}_{t+d+1:T} | \mathbf{C}_{[t+1:t+d]} = i, C_t = j, \mathbf{X}_{t-\mathbf{p}:t}) \gamma_{ji} d_i(d) \\ &= \sum_{d \in \mathcal{D}} \sum_{i \neq j} \Pr(\mathbf{X}_{t+d+1:T} | \mathbf{X}_{t+1:t+d}, \mathbf{C}_{[t+1:t+d]} = i, C_t = j, \mathbf{X}_{t-\mathbf{p}:t}) \Pr(\mathbf{X}_{t+1:t+d} | \mathbf{C}_{[t+1:t+d]} = i, C_t = j, \mathbf{X}_{t-\mathbf{p}:t}) \gamma_{ji} d_i(d) \\ &= \sum_{d \in \mathcal{D}} \sum_{i \neq q} \Pr(\mathbf{X}_{t+d+1:T} | \mathbf{X}_{t+1:t+d}, \mathbf{C}_{[t+1:t+d]} = i, C_t = j, \mathbf{X}_{t-\mathbf{p}:t}) \gamma_{ji} d_i(d) f_i(\mathbf{x}_{t+1:t+d}) \\ &= \sum_{d \in \mathcal{D}} \sum_{i \neq j} \beta_{t+d}(i) \gamma_{ji} d_i(d) f_i(\mathbf{x}_{t+1:t+d}) \end{aligned}$$

42

□

Proposition 3. Given $\beta_q^*(j) = \Pr(\mathbf{X}_{t+1:T} | C_{[t+1]} = j, \mathbf{X}_{t-\mathbf{p}:t})$, for $t = 2, \dots, T$ and $j = 1, \dots, J$

$$\beta_t^*(j) = \sum_{d \in \mathcal{D}} d_j(d) \beta_{t+d}(j) f_j(\mathbf{x}_{t+1:t+d})$$

Proof.

$$\begin{aligned}
\beta_t^*(j) &= \Pr(\mathbf{X}_{t+1:T} | C_{[t+1]} = j, \mathbf{X}_{t-\mathbf{p}:t}) \\
&= \sum_{d \in \mathcal{D}} \Pr(\mathbf{X}_{t+1:T}, C_{[t+2:t+d]} = j | C_{[t+1]} = j, \mathbf{X}_{t-\mathbf{p}:t}) \\
&= \sum_{d \in \mathcal{D}} \Pr(\mathbf{X}_{t+1:T} | \mathbf{C}_{[t+1:t+d]} = j, \mathbf{X}_{t-\mathbf{p}:t}) \Pr(C_{[t+2:t+d]} = j | C_{[t+1]} = j, \mathbf{X}_{t-\mathbf{p}:t}) \\
&= \sum_{d \in \mathcal{D}} \Pr(\mathbf{X}_{t+1:t+d}, \mathbf{X}_{t+d+1:T} | \mathbf{C}_{[t+1:t+d]} = j, \mathbf{X}_{t-\mathbf{p}:t}) d_j(d) \\
&= \sum_{d \in \mathcal{D}} \Pr(\mathbf{X}_{t+d+1:T} | \mathbf{C}_{[t+1:t+d]} = j, \mathbf{X}_{t-\mathbf{p}:t+\mathbf{p}}) \Pr(\mathbf{X}_{t+1:t+d} | \mathbf{C}_{[t+1:t+d]} = j, \mathbf{X}_{t-\mathbf{p}:t}) d_j(d) \\
&= \sum_{d \in \mathcal{D}} \Pr(\mathbf{X}_{t+d+1:T} | C_{[t+d]} = j, \mathbf{X}_{t+1+\mathbf{d}-\mathbf{p}:t+\mathbf{d}}) d_j(d) f_j(\mathbf{x}_{t+1:t+d}) \\
&= \sum_{d \in \mathcal{D}} \beta_{t+d}(j) d_j(d) f_j(\mathbf{x}_{t+1:t+d})
\end{aligned}$$

43

□

Proposition 4. *Given the definitions of $\xi_t(j)$, $\alpha_t(j)$ and $\beta_t^*(j)$, for $t = 2, \dots, T$ and $j = 1, \dots, J$*

$$\xi_t(j) = \xi_{t+1}(j) + \alpha_t(j) \sum_{i \neq j} \gamma_{ji} \beta_t^*(i) - \beta_t^*(j) \sum_{i \neq j} \alpha_t(i) \gamma_{ij}$$

44

45 *Proof.* We need the following equations for the proof

46 • $\Pr(C_t = j, \mathbf{X}_{1:T}) = \Pr(C_{t+1} = j, \mathbf{X}_{1:T}) + \Pr(C_t = j, \mathbf{X}_{1:T}) - \Pr(C_{[t+1]} = j, \mathbf{X}_{1:T})$

47 • $\Pr(C_t = i, C_{[t+1:t+d]} = j, \mathbf{X}_{1:T}) = \alpha_t(i) \gamma_{ij} d_j(d) f_j(\mathbf{x}_{t+1:t+d}) \beta_{t+d}(j)$ (Lemma 1)

48 Then

$$\begin{aligned}
\xi_t(j) &= \Pr(C_t = j, \mathbf{X}_{1:T}) \\
&= \Pr(C_{t+1} = j, \mathbf{X}_{1:T}) + \Pr(C_{[t]} = j, \mathbf{X}_{1:T}) - \Pr(C_{[t+1]} = j, \mathbf{X}_{1:T}) \\
&= \xi_{t+1}(j) + \Pr(C_{[t]} = j, \mathbf{X}_{1:T}) - \Pr(C_{[t+1]} = j, \mathbf{X}_{1:T}) \\
&= \xi_{t+1}(j) + \sum_{i \neq j} \Pr(C_{[t]} = j, C_{[t+1]} = i, \mathbf{X}_{1:T}) - \sum_{i \neq j} \Pr(C_{[t]} = i, C_{[t+1]} = j, \mathbf{X}_{1:T}) \\
&= \xi_{t+1}(j) + \sum_{i \neq j} \sum_{d \in D} \Pr(C_{[t]} = j, \mathbf{C}_{[t+1:t+d]} = i, \mathbf{X}_{1:T}) - \sum_{i \neq j} \sum_{d \in D} \Pr(C_{[t]} = i, \mathbf{C}_{[t+1:t+d]} = j, \mathbf{X}_{1:T}) \\
&= \xi_{t+1}(j) + \sum_{i \neq j} \sum_{d \in D} \alpha_t(j) \gamma_{ji} d_j(d) f_j(\mathbf{x}_{t+1:t+d}) \beta_{t+d}(i) - \sum_{i \neq j} \sum_{d \in D} \alpha_t(i) \gamma_{ij} d_i(d) f_i(\mathbf{x}_{t+1:t+d}) \beta_{t+d}(j) \\
&= \xi_{t+1}(j) + \alpha_t(j) \sum_{i \neq j} \gamma_{ji} \sum_{d \in D} d_j(d) f_j(\mathbf{x}_{t+1:t+d}) \beta_{t+d}(i) - \sum_{i \neq j} \alpha_t(i) \gamma_{ij} \sum_{d \in D} d_i(d) f_i(\mathbf{x}_{t+1:t+d}) \beta_{t+d}(j)
\end{aligned}$$

49 and finally, using that $\beta_t(j) = \sum_{i \neq j} \gamma_{ij} \beta_t^*(j)$, we have

50 $\xi_t(j) = \xi_{t+1}(j) + \alpha_t(j) \sum_{i \neq j} \gamma_{ji} \beta_t^*(i) - \beta_t^*(j) \sum_{i \neq j} \alpha_t(i) \gamma_{ij}$

51 \square

52 The following lemma was necessary to prove the previous proposition 4

Lemma 1.

$$\Pr(C_{[t]} = i, \mathbf{C}_{[t+1:t+d]} = j, \mathbf{X}_{1:T}) = \alpha_t(i) \gamma_{ij} d_j(d) f_j(\mathbf{x}_{t+1:t+d}) \beta_{t+d}(j)$$

53

Proof.

$$\begin{aligned}
\Pr(C_{[t]} = i, \mathbf{C}_{[t+1:t+d]} = j, \mathbf{X}_{1:T}) &= \Pr(C_{[t]} = i, \mathbf{C}_{[t+1:t+d]} = j, \mathbf{X}_{1:t}, \mathbf{X}_{t+1:T}) \\
&= \Pr(\mathbf{C}_{[t+1:t+d]} = j, \mathbf{X}_{t+1:T} | C_{[t]} = i, \mathbf{X}_{1:t}) \Pr(C_{[t]} = i, \mathbf{X}_{1:t}) \\
&= \Pr(\mathbf{C}_{[t+1:t+d]} = j, \mathbf{X}_{t+1:T} | C_{[t]} = i, \mathbf{X}_{1:t}) \alpha_t(i) \\
&= \Pr(\mathbf{X}_{t+1:T} | C_{[t]} = i, \mathbf{X}_{1:t}, \mathbf{C}_{[t+1:t+d]} = j) \Pr(\mathbf{C}_{[t+1:t+d]} = j | C_{[t]} = i, \mathbf{X}_{1:t}) \alpha_t(i) \\
&= \Pr(\mathbf{X}_{t+1:t+d}, \mathbf{X}_{t+d+1:T} | C_{[t]} = i, \mathbf{X}_{1:t}, \mathbf{C}_{[t+1:t+d]} = j) \gamma_{ij} d_j(d) \alpha_t(i) \\
&= \Pr(\mathbf{X}_{t+d+1:T} | C_{[t]} = i, \mathbf{X}_{1:t}, \mathbf{C}_{[t+1:t+d]} = j, \mathbf{X}_{t+1:T+d}) \\
&\quad \Pr(\mathbf{X}_{t+1:t+d} | C_{[t]} = i, \mathbf{X}_{1:t}, \mathbf{C}_{[t+1:t+d]} = j) \gamma_{ij} d_j(d) \alpha_t(i) \\
&= \Pr(\mathbf{X}_{t+d+1:T} | C_{[t+d]} = j, \mathbf{X}_{t+1:T+d-1}) \Pr(\mathbf{X}_{t+1:t+d} | \mathbf{X}_{t+1:T+d-1}) \gamma_{ij} d_j(d) \alpha_t(i) \\
&= \beta_{t+d}(j) f_j(\mathbf{x}_{t+1:t+d}) \gamma_{ij} d_j(d) \alpha_t(i)
\end{aligned}$$

55 **2.2 From Global Decoding section**

Proposition 5. Be

$$\psi_t(j, d) = \max_{c_{1:t-d}} \Pr(\mathbf{C}_{1:t-d}, \mathbf{C}_{[t-d+1:t]=j}, \mathbf{X}_{1:T})$$

56 for $t = 2, \dots, T$, $d = 1, \dots, D$ and $j = 1, \dots, J$, then

$$\psi_t(j, d) = \max_{\substack{i \neq j \\ d' \leq t}} \{\psi_{t-d}(i, d') \gamma_{ij} d_j(d) f_j(\mathbf{x}_{t-d+1:t})\}$$

Proof. By definition we have

$$\psi_{t-d}(i, d') = \max_{c_{1:t-d-d'}} \Pr(\mathbf{C}_{1:t-d-d'}, \mathbf{C}_{[t-d-d'+1:t-d]} = i, \mathbf{X}_{1:t-d})$$

In the same way,

$$\begin{aligned} \psi_t(j, d) &= \max_{c_{1:t-d}} \Pr(\mathbf{C}_{1:t-d}, \mathbf{C}_{[t-d+1:t]} = j, \mathbf{X}_{1:t}) \\ &= \max_{\substack{c_{1:t-d-d'} \\ c_{t-d-d'+1:t-d} \\ d' \leq d}} \Pr(\mathbf{C}_{1:t-d-d'}, \mathbf{C}_{t-d-d'+1:t-d}, \mathbf{C}_{[t-d+1:t]} = j, \mathbf{X}_{1:t-d}, \mathbf{X}_{t-d+1:t}) \\ &= \max_{\substack{c_{1:t-d-d'} \\ i \neq j \\ d' \leq d}} \Pr(\mathbf{C}_{1:t-d-d'}, \mathbf{C}_{[t-d-d'+1:t-d]} = i, \mathbf{C}_{[t-d:t]} = j, \mathbf{X}_{1:t-d}, \mathbf{X}_{t-d+1:t}) \\ &= \max_{\substack{c_{1:t-d-d'} \\ i \neq j \\ d' \leq d}} \Pr(\mathbf{C}_{1:t-d-d'}, \mathbf{C}_{[t-d-d'+1:t-d]} = i, \mathbf{X}_{1:t-d}) \gamma_{ij} d_j(d) \Pr(\mathbf{X}_{t-d+1:t} | \mathbf{X}_{t-d+1:t} \mathbf{X}_{t-d+1:t}) \\ &= \max_{\substack{c_{1:t-d-d'} \\ i \neq j \\ d' \leq d}} \Pr(\mathbf{C}_{1:t-d-d'}, \mathbf{C}_{[t-d-d'+1:t-d]} = i, \mathbf{X}_{1:t-d}) \gamma_{ij} d_j(d) f_j(\mathbf{x}_{t-d+1:t}) \\ &= \max_{\substack{i \neq j \\ d' \leq d}} \psi_{t-d}(i, d') \gamma_{ij} d_j(d) f_j(\mathbf{x}_{t-d+1:t}) \end{aligned}$$

58 3 RMSE extra figure

59 In order to measure the predictive capacity of the models proposed when analyse the accelerometer sheep
 60 data, the Root Mean Squared Error (RMSE) was calculated over the four model: AR(1)-HMM, HMM,
 61 AR(1)-HSMM and HSMM. For each observed time series and model, using a 100 sample of the fitted
 62 posterior, we computed 100 predictions (using the FB algorithm) of the hidden states and the observation
 63 process. Figure 1 shows the values obtained

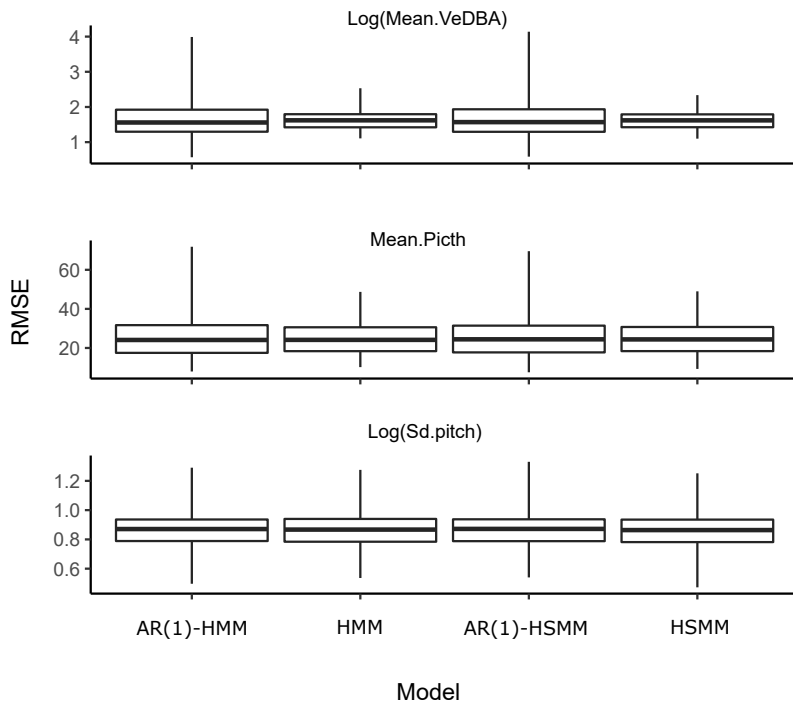


Figure 1: Boxplots of the Root Mean Squared Error over the observations for the four models considered.